Talanta 92 (2012) 26–37

Contents lists available at SciVerse ScienceDirect

Talanta

journal homepage: www.elsevier.com/locate/talanta

A novel in-line NIR spectroscopy application for the monitoring of tablet film coating in an industrial scale process

C.-V. Möltgen[a], T. Puchert[a], J.C. Menezes[b], D. Lochmann[c], G. Reich[a,*]

[a] Institute of Pharmacy and Molecular Biotechnology, Department of Pharmaceutical Technology and Biopharmaceutics, University of Heidelberg, Im Neuenheimer Feld 366, 69120 Heidelberg, Germany
[b] Institute for Biotechnology and Bioengineering, IST, Technical University of Lisbon, Portugal
[c] Quality Operations, PAT – Laboratory, Merck Serono, Darmstadt, Germany

ARTICLE INFO

Article history:
Received 28 July 2011
Received in revised form 1 December 2011
Accepted 4 December 2011
Available online 31 January 2012

Keywords:
Process Analytical Technology (PAT)
Film coating
Near-Infrared Spectroscopy (NIRS)
In-line monitoring
NIR Chemical Imaging (NIR-CI)
Multivariate Data Analysis (MVDA)

ABSTRACT

Film coating of tablets is a multivariate pharmaceutical unit operation. In this study an innovative in-line Fourier-Transform Near-Infrared Spectroscopy (FT-NIRS) application is described which enables real-time monitoring of a full industrial scale pan coating process of heart-shaped tablets. The tablets were coated with a thin hydroxypropyl methylcellulose (HPMC) film of up to approx. 28 μm on the tablet face as determined by SEM, corresponding to a weight gain of 2.26%. For a better understanding of the aqueous coating process the NIR probe was positioned inside the rotating tablet bed. Five full scale experimental runs have been performed to evaluate the impact of process variables such as pan rotation, exhaust air temperature, spray rate and pan load and elaborate robust and selective quantitative calibration models for the real-time determination of both coating growth and tablet moisture content. Principal Component (PC) score plots allowed each coating step, namely preheating, spraying and drying to be distinguished and the dominating factors and their spectral effects to be identified (e.g. temperature, moisture, coating growth, change of tablet bed density, and core/coat interactions). The distinct separation of HPMC coating growth and tablet moisture in different PCs enabled a real-time in-line monitoring of both attributes. A PLS calibration model based on Karl Fischer reference values allowed the tablet moisture trajectory to be determined throughout the entire coating process. A 1-latent variable iPLS weight gain calibration model with calibration samples from process stages dominated by the coating growth (i.e. ≥30% of the theoretically applied amount of coating) was sufficiently selective and accurate to predict the progress of the thin HPMC coating layer. At-line NIR Chemical Imaging (NIR-CI) in combination with PLS Discriminant Analysis (PLSDA) verified the HPMC coating growth and physical changes at the core/coat interface during the initial stages of the coating process. In addition, inter- and intra-tablet coating variability throughout the process could be assessed. These results clearly demonstrate that in-line NIRS and at-line NIR-CI can be applied as complimentary PAT tools to monitor a challenging pan coating process.

1. Introduction

Tablet coating is a multivariate unit operation with various process parameters, i.e. spray rate, inlet- and exhaust air temperature, inlet- and exhaust air flow, atomization air pressure, pan speed and gun to bed distance. Since spraying, distribution and drying of the coating formulation take place at the same time, tablet coating growth and uniformity are affected by many Critical Process Parameters (CPPs). A change of the gun spray rate has a significant effect on the time needed to get a certain amount of coating on the tablet [1]. The inlet- and exhaust air temperature and also the spray rate are important factors of the film formation from aqueous polymeric dispersions, thus contributing to the final product performance. As the coalescence occurs only at a certain temperature, i.e. the minimum film formation temperature and a specific moisture content [2], these CPPs have to be monitored and optimized. Moreover, a homogeneous droplet size and a defined droplet velocity are important parameters for a good coating quality. Both parameters are affected by the atomization air pressure and also by the gun to bed distance [3]. The impact of the atomization air pressure on film coat surface roughness was investigated by Twitchell [4] and Perfetti et al. [5]. A low surface roughness can be achieved with a higher atomization air pressure, which leads to a higher velocity of the droplets and thus to an increased droplet spreading resulting in a smoother coating.

The current approach of coating process monitoring and end point determination is based on collecting samples from the coater. Tablet weight gain is mostly used to verify the amount of

* Corresponding author. Tel.: +49 6221 54 8335; fax: +49 6221 54 5971.
E-mail address: Gabriele.Reich@urz.uni-heidelberg.de (G. Reich).

0039-9140/$ – see front matter © 2012 Elsevier B.V. All rights reserved.
doi:10.1016/j.talanta.2011.12.034

coating on the collected samples and determine the process endpoint. For aqueous based non-functional coatings, tablet moisture content can be an additional quality attribute to be assessed. The average film coat thickness is often calculated from the applied mass of coating liquid. For functional coatings, indirect methods such as disintegration or dissolution tests are applied to verify the thickness and homogeneity of the coating layer. All these methods are time-consuming and mostly destructive. To improve process efficiency and ensure consistent product quality according to QbD principles [6–8], timely measurements are required enabling CPPs and Critical Quality Attributes (CQA) to be monitored [9]. Near-Infrared Spectroscopy (NIRS) is one of the techniques that have been described for coating process monitoring and endpoint determination [10,11]. NIRS has been applied off-line [12,13], at-line [14,15], and in-line in a fluidized bed apparatus [16–18] and in a pan coater [19–21]. Peréz-Ramos et al. [19] developed a NIRS method for in-line analysis of tablet film coating thickness in a lab scale pan coater. An empirical geometric 2-vector volumetric growth model was developed to account for the differential growth on the face and band regions of biconvex tablets. The mean coating layer thickness was up to 180 microns (μm) in the face region and 135 μm in the band region. The correlation between values estimated from NIR data and off-line measurements of the volumetric growth in tablets gave good results. Römer et al. [20] developed a calibration model based on NIRS data obtained from a small scale rotating plate coating system that can be used for the prediction of coating layer thickness of tablets coated in a drum coater. The measured average coating thickness ($n = 100$ tablets) was 210 μm. Gendre et al. [21] performed in-line NIRS measurements in a small scale pan coater using a photodiode array spectrometer to monitor the coating process. A functional aqueous based polymer combination was used as coating material. PLS models were developed for the prediction of the mass of coating material and the film thickness using two different reference methods namely weighing and terahertz pulsed imaging (TPI). The models provided accurate NIR predictions. A coating thickness range of 60 and 170 μm and a mass range of 11 and 35 mg were determined.

Coating quality assessment requires information not only on the average coating mass or the average coating layer thickness of a tablet batch, but also on inter-tablet variability of the coating thickness or its uniformity on each individual tablet. A lengthy and destructive method that has been applied to visually determine micro heterogeneities of tablet coatings is scanning electron microscopy (SEM) [22]. An autofluorescent agent in the coating layer is required to use confocal laser scanning microscopy (CLSM) for this purpose [18,23]. Non-destructive techniques for chemical visualisation of film coat thickness and micro heterogeneities include attenuated total reflection-infrared (ATR-IR) imaging [24], NIR Chemical Imaging (NIR-CI) [25] and terahertz pulsed imaging (TPI) [25,26]. TPI allows a direct coating thickness determination over the whole tablet surface. However, the thinnest coating layer that could be precisely quantified using TPI was about 40 μm [26]. ATR-IR imaging and NIR-CI are indirect methods which use changes in absorbance values for coating layer determination. Due to the larger field-of-view of NIR-CI, which enables the visualization of sample areas as large as 40 mm × 32 mm, whole tablet coating analysis is significantly faster compared to ATR-IR imaging. Moreover, the higher penetration depth allows information to be obtained from core and coat, simultaneously. The advantage of NIR-CI over TPI is the lower detection limit and the higher spatial resolution. The spatial resolution of TPI is physically limited due to the diffraction limit caused by the longer wavelength of the THz radiation (0.03–3 mm) and due to the device optics. Since operating at shorter wavelengths provides a higher axial resolution, a better detection of thin coatings can be expected with NIR-CI [25,26].

To the best of our knowledge, there have been no reports on in-line NIR process monitoring to determine the growth of very thin tablet coatings in a full industrial scale pan coater and its verification with at-line NIR-CI. The aim of the present study was to monitor simultaneously throughout the process the growth of a very thin HPMC coating layer on heart-shaped tablets (up to 28 μm on the tablet face) and the tablet moisture trajectory. This latter aspect is of great importance for the quality of the final product, since the tablet cores can take up water from the aqueous coating solution. As temperature and moisture are known to have a significant influence on the spectra [27], measurements above the tablet bed were supposed to be affected by the air temperature and the evaporation of the fine spray (i.e. water) coming from the spray nozzles. To reduce these effects, the NIR probe was positioned inside the tablet bed. An FT-NIR spectrometer was selected because of its speed and spectra reproducibility. The sensitivity of the analyzer to changing operation parameters was tested with the goal, to understand the impact of CPPs such as spray rate and exhaust air temperature on the spectra and the product properties. In addition, the potential of NIR-CI as an at-line PAT tool to verify the coating growth and analyze inter- and intra-tablet coating variability during the coating process was evaluated.

2. Materials and methods

2.1. Materials

2.1.1. Tablets

The uncoated, heart-shaped tablets (average core weight of 169 mg) contained an active pharmaceutical ingredient (API) and four excipients (microcrystalline cellulose, corn starch, crospovidone and magnesium stearate).

2.1.2. Coating formulation

The tablet cores were coated with an aqueous coating formulation, consisting of 60% hydroxypropyl methylcellulose (HPMC) as film forming polymer, macrogol as plasticizer and lower amounts of titanium dioxide, iron(III) oxide and dimeticon.

2.2. Methods

2.2.1. Experimental design

The tablets were film coated using an industrial scale perforated pan coater (GC 1000, Glatt®) connected to a peristaltic pump (Watson Marlow® 604U). Tablet samples were withdrawn through a small separate door inside the main door of the coater using a flexible tube connected with an aspirator. Samples were collected during the whole coating process i.e. the preheating-, the spraying- and the drying-phase. During spraying the allocation of samples was in 10% levels of the theoretically applied coating formulation. This resulted in samples of cores, while preheating, at 10–100% spraying, and of the finished product (i.e. total of 14 samples). The theoretically applied amount of coating per tablet at the 100% level was 3.83 mg corresponding to a weight gain of 2.26% of the core tablet weight.

The coating conditions for each individual run are summarized in Table 1. Coating parameters not mentioned in the table were kept constant. The pan rotation speed which was set at 11 rounds per minute (rpm) during the “preheating”, “pan rotation with T” and the “spraying” step and 6 rpm during the “drying” step. Sampling details are given in Table 2.

Five runs (A1, A2, B1, B2, C) of in-line experiments were investigated. The runs A1 and A2 comprised coated tablets to evaluate the effect of changing process parameters, namely exhaust air temperature and spray rate on the NIR spectra.

Table 1
Process parameters of all experimental in-line runs.

Run	Cores (−) or coated tablets (+)	Process variables			Target parameters
		Pan load [kg]	Spray rate S1[a]/S2[a]/S3[a] [ml/min]	Exhaust air temperature [°C]	
A1	+	150	200/160/n.a.[b]	25–70	Temperature effect
A2	+	150	200/160/200	25–50	Spray rate effect
B1	–	130	220/160/n.a.	45	Density and tablet motion
B2	–	130	220/160/n.a.	45	Density and tablet motion
C	–	150	220/160/n.a.	45	Coating growth and moisture

[a] S1 = spraying 1; S2 = spraying 2; S3 = spraying 3.
[b] n.a. = not applied.

Table 2
Schematic presentation of the different sampling ranges for PLS modeling.

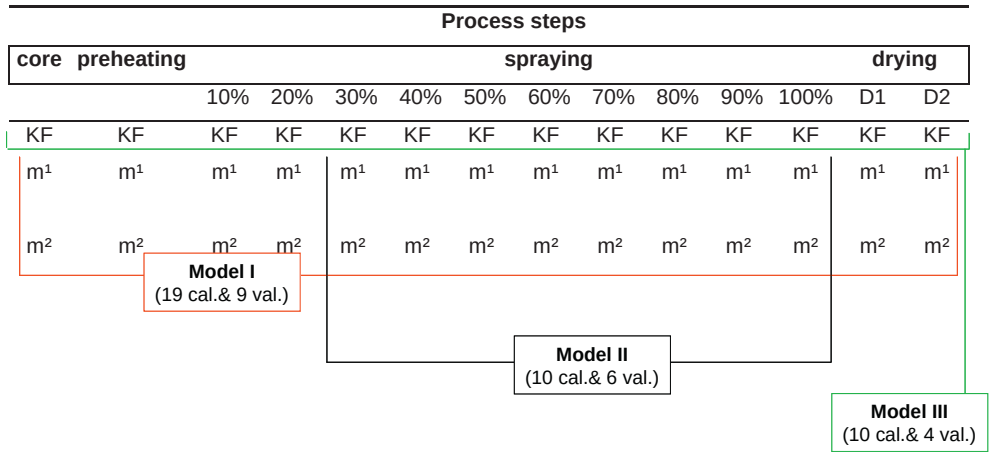

KF = Karl Fischer value.
m1 = mean value #1 (mean value of 100 tablet weights).
m2 = mean value #2 (mean value of 100 tablet weights).
D1, D2 = drying 1, drying 2.

Both runs started with a step named "pan rotation without T" in which the tablets were moved without any preheating, followed by the preheating, i.e. "pan rotation with T" step, the spraying steps and the drying step.

Three in-line runs (B1, B2, C) were performed with uncoated tablet cores. The coating process was monitored at all steps, starting from the "preheating" step throughout the "spraying 1 and 2" steps and the drying step. In all three runs (B1, B2, C) the same settings were used for each coating step. The only difference was the process time being longer for run (C) because of the higher pan load (Table 1). In the runs (B1 and B2) differences in tablet density and tabled bed motion during the coating process were investigated. Run (C) was performed to develop quantitative calibration models based on weight gain and Karl Fischer reference data to monitor both the growth of the thin coating layer and also the process trajectory of tablet moisture.

2.2.2. In-line Near-Infrared Spectroscopy

As outlined before the NIR diffuse reflectance spectra were collected from inside the rotating tablet bed of a pan coater. Spectra acquisition was performed with a FT-NIR spectrometer (Matrix-F®, Bruker Optik GmbH, Ettlingen Germany) combined with a reflection-immersion probe (Reflector Flush®, Solvias). Additionally, the system was equipped with a gas rinsing nozzle that enables cleaning of the optical Sapphire window without removing the nozzle from the tablet bed. The Matrix-F is equipped with a tungsten-halogen source and an InGaAs detector. NIR in-line spectra were continuously obtained in the range of 4000–12800 cm^{-1} with a sample size of approx. 10 tablets per scan, a resolution of 36 cm^{-1} and 66 scans per spectrum. In addition, we set the mirror velocity at 40 kHz for more scans at the same time. One accumulation of spectra took 4.1 s. The optimal settings of the analyzer were determined with the methodology of Design of Experiments (DoE) (data not shown). For performing and analyzing the experimental series in a systematic and efficient way a D-optimal Design was chosen. The setup and the positioning of the NIR reflectance analyzer inside the pan coater is shown in Fig. 1.

2.2.3. Multivariate Data Analysis

The OPUS® software (Bruker Optik, Ettlingen Germany) was used for data acquisition. Further Multivariate Data Analysis was performed with Simca-P+® v.12.0 (Umetrics AB, Ulmeå Sweden). The interval partial least-squares (iPLS) algorithm [28] was per-

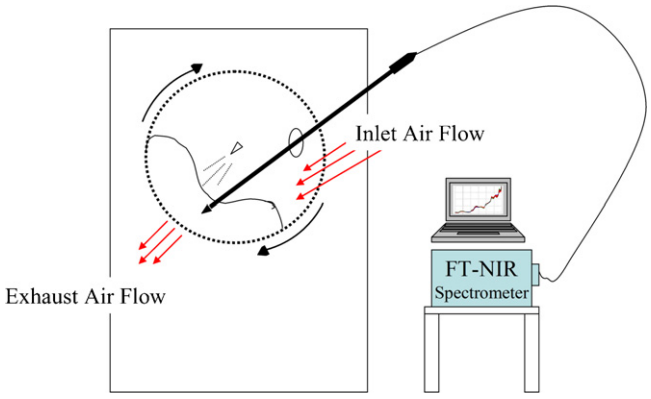

Fig. 1. Instrumental setup for in-line NIRS coating monitoring.

formed using Matlab® R2010a v.7.10 (Mathworks, Inc., USA) with PLS toolbox® v.6.0 (Eigenvector Research Inc., USA). The collected NIR spectra were used in the wavenumber range of 10,506.9–4520.6 cm^{-1}. The spectral data were analyzed with pre-processing techniques, i.e. multiplicative scatter correction (MSC) [29] and mean centering to improve the quality of the models. Principal Component Analysis (PCA) and Partial Least Squares (PLS) regression were used to build qualitative and quantitative models, respectively. PCA is an unsupervised variable reduction technique being used for constructing new variables, known as Principal Components (PC). The quantitative models for tablet weight gain and tablet moisture were developed with the iPLS algorithm as a variable selection methodology. The principal of iPLS is to split the spectra into a given number of equidistant subintervals and develop PLS-1 regression models for each subinterval. Cross-validation is performed for each of these models and the subinterval which provides the lowest model root-mean-square error of cross-validation (RMSECV) is selected. The optimal subinterval can be found by adding or subtracting new variables. This approach indicated the wavelength region from 5646 cm^{-1} to 5508 cm^{-1} as the best for the calculation HPMC coating growth based on tablet weight reference values. The most selective region for water was calculated in the wavelength range of 5492–4998 cm^{-1}. The accuracy of the models was evaluated by comparing the in-line NIR data with those of the reference methods, e.g. analytical balance and Karl Fischer titration according to the following criteria: the correlation coefficient (R^2), the root mean square error of calibration (RMSEC), the root mean square error of cross validation (RMSECV), and the root mean square error of prediction (RMSEP).

2.2.4. Near-Infrared Chemical Imaging

Tablet samples collected during the spraying phase were analyzed for coating growth and coating distribution using a SyNIRgi® Chemical Imaging System (Malvern Instruments, Malvern, UK) equipped with an InSb focal plane array detector (320 × 256 pixel) and a 25-position automatic sample holder. To get a representative sampling both faces of each tablet were measured. For each spraying stage (i.e. 10–100%) 20 tablets were analyzed. This resulted in 400 images. Imaging was not possible on the centerband because of the tablet shape and the strong curvature of the round parts, which made identical positioning of each tablet difficult. Image cubes of tablet samples at each coating level were acquired with Pixys® 1.1 software (Malvern Instruments, Malvern, UK) in the spectral range 1200–2400 nm with a spectral resolution of 10 nm and 16 frames per wavelength. The field of view was set to 12.8 × 10.2 which encompasses 100% of the area of the sample and provides a magnification of 40 μm per pixel. Each image cube contained 81,920 full NIR spectra and required a collection time of approximately 3 min. Before the sample was scanned, it was necessary to accomplish a dark response and a background correction because the intensity of the raw signal from the sample is also influenced by the system components. After this reference correction the instrumental influences are characterized in the "background". The correction of the raw data was performed according to the following equation (1):

$$\mathrm{Cube}_{\mathrm{Final}} = \left(\frac{\mathrm{Cube}_{\mathrm{Sample}} - \mathrm{Cube}_{\mathrm{Dark}}}{\mathrm{Cube}_{\mathrm{Background}} - \mathrm{Cube}_{\mathrm{Dark}}} \right) \quad (1)$$

This calculation was performed for all pixels in all planes in the cube. Data were analyzed using ISys® software (Malvern instruments Ltd., Malvern, UK). Before the image pre-processing algorithms were applied all spectra were converted to absorbance unit. The regions around the tablets were masked with the threshold image function. The data were pre-processed using a standard normal variate (SNV) algorithm and a first derivative. A Savitzky–Golay filter was calculated using third-order polynomials each 19 data points long. The hyperspectral reference library was built for the core and the HPMC with more than 600 spectra per component. The spectral data were computed in the same way. For the determination of coating growth partial least squares discriminant analysis (PLSDA) was performed. The PLS-2 predicted images are associated with histogram plots, which were used to perform sample statistic. One parameter given by the histogram is the mean value which was used to accomplish an Analysis of Variance (ANOVA).

2.2.5. Reference methods

For the determination of tablet weight gain and tablet moisture content samples were studied with two reference methods, namely an analytical balance (Mettler, AT 261 Delta Range® FACT) and Karl Fischer titration. The reference values for the multivariate models were determined as follows: for each coating step (i.e. core, preheating, 10–100% spraying and two times during drying) 20 sets of 10 tablets were weighted. Then two mean values of 100 tablets each was calculated, resulting in a total of 28 tablet weights. Two PLS calibration models (model I, model II) with mean reference values from two different sampling ranges were developed both using the same wavelength region calculated by iPLS. In addition, an iPLS calibration model (model III) for tablet moisture content was determined using Karl Fischer reference values. The moisture determination was performed using an Oven Sample Processor 774 with a KF Coulometer 831 (Methrom, Fliederstadt, Germany). Each weighted sample containing 10 crushed tablets was preheated in the oven. The evaporated water from the sample was transported by a dry carrier gas to the titration cell. The analysis was performed with iodide KF Coulometric reagent CombiCoulomat fritless (Merck, Darmstadt, Germany) and Lactose standard 5% (Merck, Darmstadt, Germany). The calibration and validation samples are specified in Table 2.

Scanning Electron Microscopy (SEM) (Leo/Zeiss Supra 35®, Carl Zeiss, Oberkochen, Germany) and Energy Dispersive X-ray (EDX) Spectroscopy were used to determine the coating layer thickness and the surface characteristics of the film coated tablets. One tablet of each spraying stage (i.e. 10–100%) was investigated at different locations on the face and the band region, respectively. Then the average coating thickness of the tablet face and the tablet band was calculated at each spraying stage. For sample preparation, the tablets were divided at the score lines into two halves. Each half was fixed onto a special sample holder. Then they were sputtered with platinum using a vacuum evaporator. SEM images were obtained at an acceleration voltage of 5.0 kV. EDX was used for the detection of iron(III) included in the coating solution for a better distinction between core and coating.

3. Results and discussion

Performing in-line NIRS measurements in a pan coating process reveals spectral changes resulting from process-induced changes of core properties, coating growth and different moisture conditions. Fig. 2 shows the spectral changes during the pan coating process. The intensity of the NIR signal corresponding to HPMC strongly increased during the spraying phase. The spectral similarity between coated tablets and the HPMC raw material indicates that the spectral information of the coating formulation is dominated by HPMC. HPMC has a characteristic intense NIR band region between 5800 cm^{-1} and 5500 cm^{-1} which corresponds to the first overtone of the CH-stretching vibration of the polymer backbone. Water bands can be monitored at 6835 cm^{-1} and at 5190 cm^{-1} which correspond to the first overtone of the OH-stretching vibration and the combination band of OH of core and coat components.

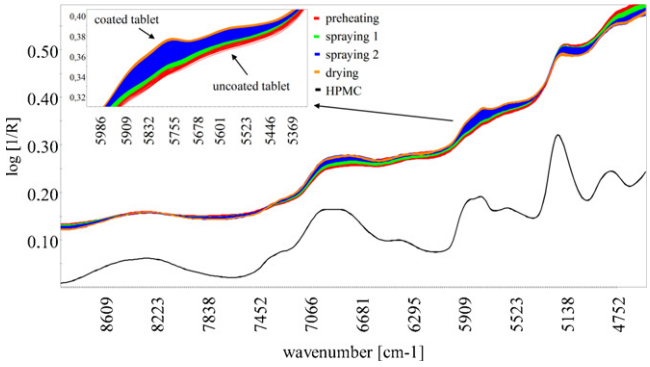

Fig. 2. NIR reflectance spectra of the coating process – increase of absorbance values between 5986 cm^{-1} and 5369 cm^{-1} show the effect of HPMC film growth. (For interpretation of the references to colour in this figure legend, the reader is referred to the web version of the article.)

3.1. Qualitative in-line NIR monitoring

Four experiments (A1–A2, B1–B2) were performed to study the influence of different process variables (see Table 1) on the NIR spectra and related product properties.

Fig. 3a illustrates a PC score plot of 1170 reflectance NIR spectra for the first experimental run (A1). Each spectrum was pretreated by MSC for compensation of scatter-induced baseline shifts and intensity differences. Some correlations with the operation variables can be found in the score plot. Arrows are added to the plot to describe these correlations. The scores are clustered according to each coating step, i.e. different process parameters affected the tablet properties, which in turn were detected by NIRS. The experiment started with a "pan rotation without T" step. During this step the tablets were rotated in the pan at room temperature. The cluster shows that the rotation of coated tablets has little influence on the NIR measurements. Then the increase of temperature can be observed. During normal pan rotation speed the coater was heated up to 50 °C, 65 °C and then 70 °C by increasing the exhaust air temperature. Fig. 3b shows the spectral changes during the "pan rotation with T" step. A shift and an intensity decrease of the combination band of OH stretching vibrations, indicating changes in water content are clearly visible. After cooling down the exhaust air temperature to 50 °C the first spraying step started and the temperature decreased to 45 °C. Interestingly, there is no separation of the scores between the "pan rotation with T" step and the "spraying 1" step, indicating that temperature-induced changes and their effect on the spectra were more pronounced than the effect of the additional coating growth. This may be attributed to the fact that in this run (A1) the tablets were already coated from the beginning of the experiment and the "spraying 1" step was short. The loadings plot in Fig. 3c verified the dominating temperature effect on the OH bonds in the first PC. In "spraying 2" the spray rate was reduced at constant temperature (45 °C) which is also visible in the score plot (Fig. 3a). The score clusters of "spraying 1" and "spraying 2" differ clearly in their direction. This indicates that in "spraying 2" moisture and coating growth are dominating the spectral information, which is also shown in the loadings plot of PC 2 (Fig. 3c). After spraying, the "drying" step took place and shows the same trend as the "pan rotation with T" step. Based on this experiment it was shown that the pan rotation is not a disturbing factor. On the other hand, the spectral effects of changes in process parameters such as exhaust air temperature and spray rate are directly visible, i.e. may not be neglected.

In the second experiment (A2) the spray rate was varied. 1160 reflectance NIR spectra were collected during this run. Due to a lower temperature and a shorter period of the "pan rotation with

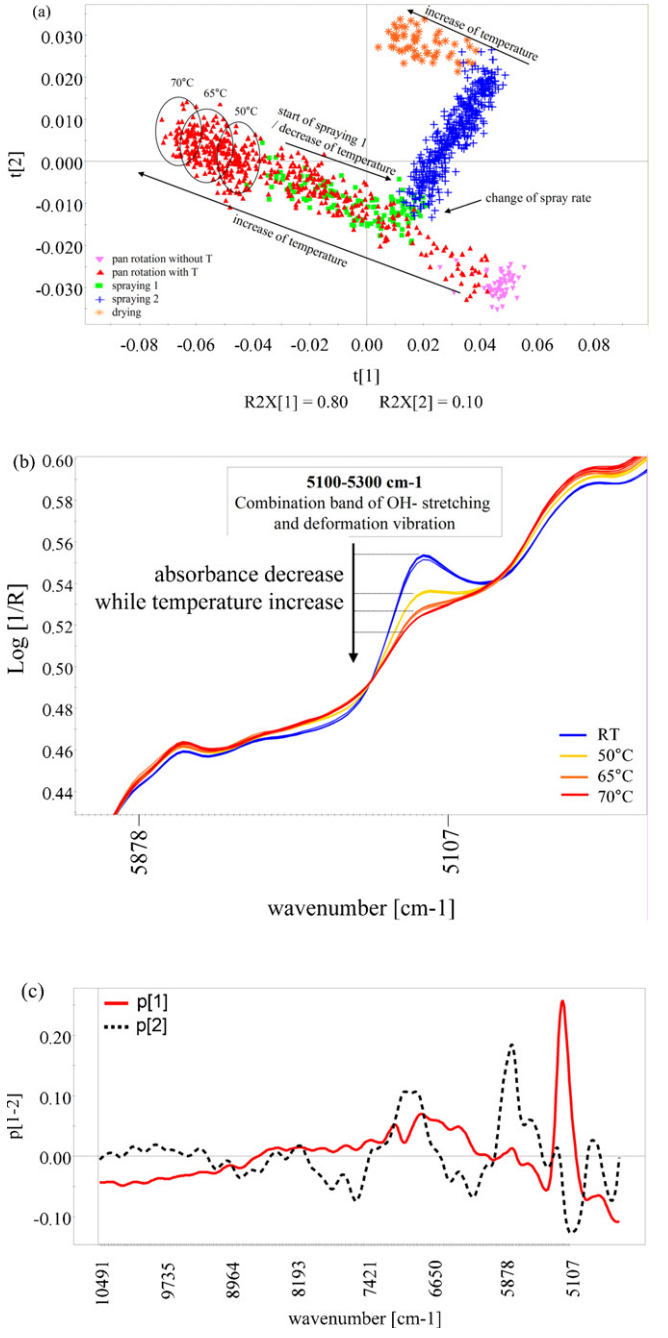

Fig. 3. (a) PC score plot of the first experimental run (A1). The scores are clustered according to each coating step. (b) Temperature induced spectral changes during the "pan rotation with T" step, spectra are shown after pre-processing using MSC. (c) Corresponding loadings plot of PC 1 and PC2.

T" step compared to A1, the temperature effect on the spectra was less pronounced and the coating growth was explained by the first PC. The trajectory of the tablet moisture content during the process is shown in a score line plot of the second PC (Fig. 4a). As illustrated in Fig. 4b, the loading of this PC verifies the moisture information.

The changes of the spray rate are directly visible. In the "pan rotation without T" step the already existing moisture level of the tablets was more or less the same, but when the temperature increased there was a distinct decrease of the tablet moisture content. After starting the first spraying step with 200 ml/min the moisture content increased and slightly decreased again when the spray rate changed to 160 ml/min at constant temperature. By increasing the spray rate again to 200 ml/min the change of the

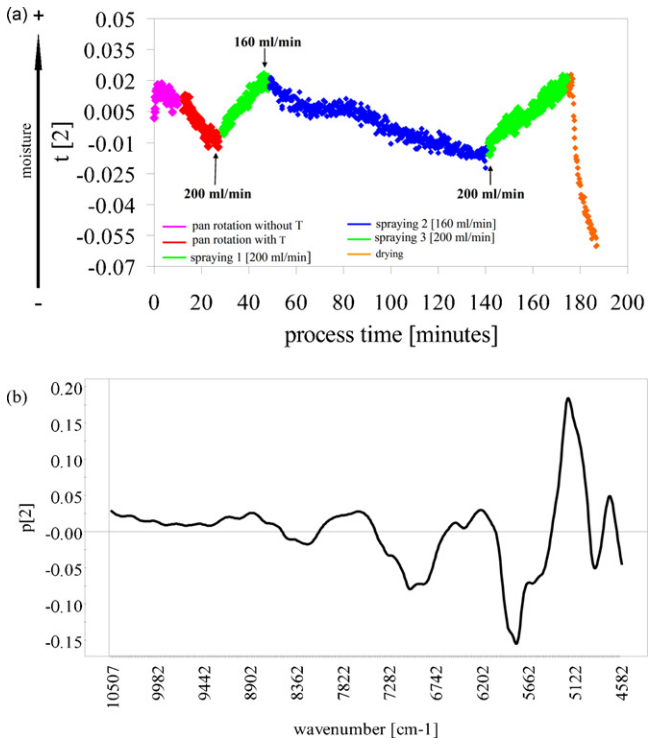

Fig. 4. (a) PC score line plot of the moisture progress during the entire coating process of the second experimental run (A2). (b) Loading plot of PC 2. (For interpretation of the references to colour in this figure legend, the reader is referred to the web version of the article.)

moisture content is also recognizable. Finally, during "drying" the moisture decreased to a minimum as expected. Thus, it can be concluded that the distinction of the tablet moisture content from the coating growth and other process related spectral features is feasible.

The runs B1 and B2 have been performed to evaluate the sensitivity of in-line NIRS measurements to tablet density differences and changes in tablet bed motion, which may occur during a pan coating process after a certain amount of coating material has been applied. For this purpose, we used cores instead of pre-coated tablets and decreased the pan load to 130 kg (see Table 1). During "preheating" and at the early stage of "spraying 1", all the NIR measurements occurred within the tablet bed. At the end of the first spraying step, the volume of the tablet bed decreased and as a result, the NIR analyzer slipped out of the tablets and measured in the gas phase mainly consisting of evaporated water. A drawback of the proposed application is the limitation in the positioning the probe in the tablet bed due to the fixed baffles at the pan wall. Thus, the immersion depth of the probe cannot be adapted to a decreased volume of the tablet bed.

For data analysis a PCA model was generated to summarize the main variation in the complete data set. The data set consisted of 2138 reflectance NIR spectra. Fig. 5 presents the score line plots of the first PC scores which show how the processes B1 and B2 proceeded over time.

Both experiments (B1–B2) reveal the same trajectory. The scores from the "preheating" step show variations as seen before in Fig. 3. The variation reveals the temperature effect which declines after starting "spraying 1". At the end of this spraying step, i.e. after approx. 32 min of process time strong fluctuations are observed during the second spraying step. These fluctuations were caused by the decrease of the tablet bed volume after a certain time which is an indicator for a defined amount of coating material applied to the tablets. This change of the tablet bed volume, which often happens in full industrial scale pan coaters, also implicates a change of the distance and the angle of the analyzer to the tablet bed. Sometimes, even the spray arm, where the several spray nozzles are mounted, has to be corrected by the operator. A shift in spray gun to bed distance may have an influence on the coating quality, since a greater distance intensifies the influence of the viscosity on the droplet size and influences the droplet velocity. The spray width and height of the spray zone are also affected [3]. As indicated in Fig. 5, three steps can be observed within the second spraying phase. The volume of the tablet bed decreased after 20% of spraying. Tablet coating was unsteady and incomplete. Thus, the strong spectral fluctuations in the beginning of the second spraying step can be explained by changes in the surface properties and the moisture content of the tablets and the overall tablet bed density, affecting the reflectance characteristics, i.e. the penetration depth of the NIR light and the path length to the tablets and back to the sensor. Reduced spectral variations are observed at the end of "spraying 2",when the motion of the tablet bed is more consistent and the tablet coating gets more uniform and complete. The knowledge at what particular time the change of the tablet bed volume takes place can be used as a good indicator. A too wet tablet bed could be detected at an early stage and would enable a rapid intervention in the process.

3.2. Quantitative in-line NIR monitoring

In run (C) the quantitative determination of coating growth and tablet moisture content was elaborated.

Fig. 6a displays a PC score plot of 1367 NIR reflectance spectra. The data were mean centered and pre-processed by MSC. The plot illustrates the first and the second PC. The grouping of the scores in clusters is easily visible and shows again that a change of the tablet characteristics has happened during the process. As seen before the temperature effect in the "preheating" step is shown by the disorder of scores. As soon as the "spraying 1" step starts the scores

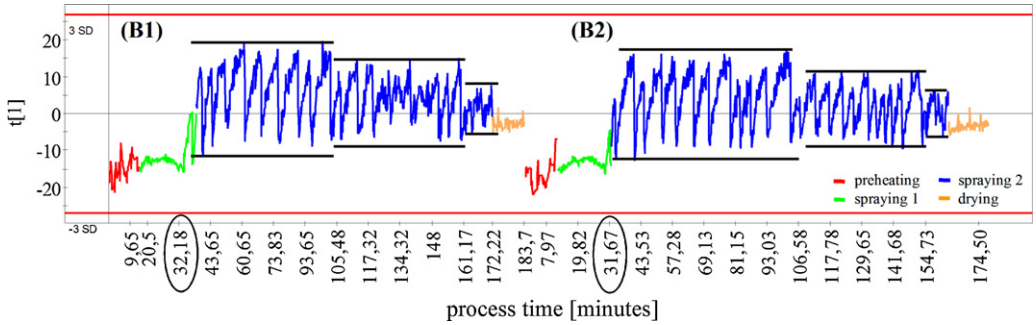

Fig. 5. PC score line plots of two monitoring runs (B1–B2) over process time – decrease of the tablet bed volume after around 32 min. (For interpretation of the references to colour in this figure legend, the reader is referred to the web version of the article.)

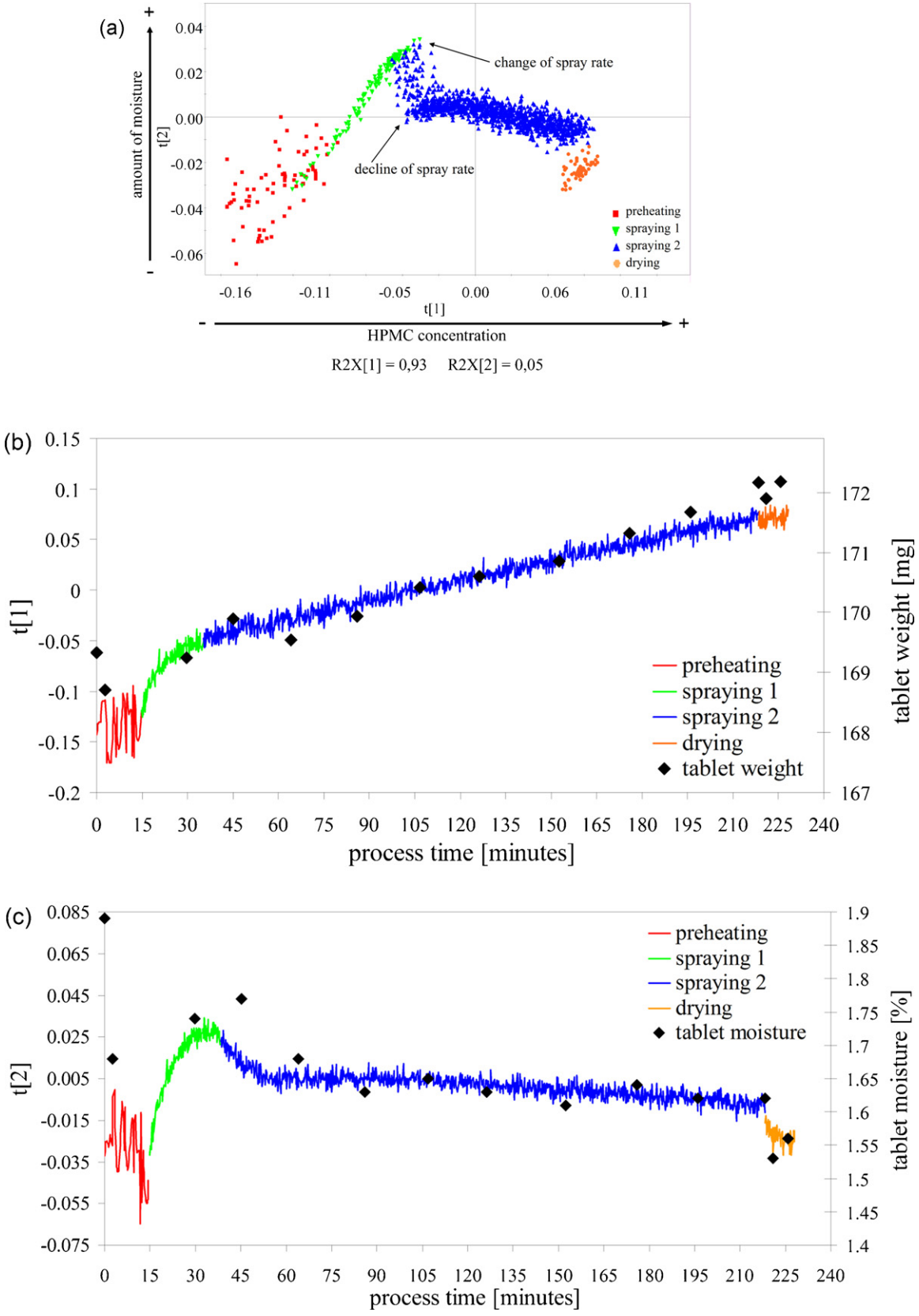

Fig. 6. (a) PC score plot of run C; (b) score line plot of PC 1 indicating the coating growth and mean tablet weights at each process step; (c) score line plot of PC 2 indicating the tablet moisture trajectory and Karl Fischer values at each process step; (d) corresponding loadings plot of PC1 and PC2 and the NIR raw spectrum of HPMC for comparison. (For interpretation of the references to colour in this figure legend, the reader is referred to the web version of the article.)

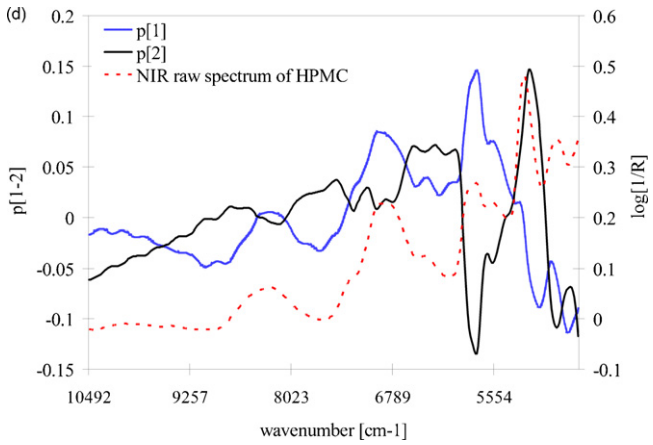

Fig. 6. (*Continued*)

are in order of time and the separation between these two steps is observable. The change of the spray rate in the second spraying step is marked by another clustering direction of the scores. During this run it happened that in "spraying 2" the spray rate was not constant at 160 ml/min. It declined to 150 ml/min. This was not planned but it could be monitored immediately in the spectra. This event emphasizes that not estimated changes in process parameters and related changes in product characteristics can be identified and eventually corrected in time. After spraying took place, the scores of the "drying" step are represented by a separate cluster because of different moisture information.

The first PC explains with 93% variation the concentration of HPMC and the second PC accounts for 5.2% variation and is related to the moisture content.

For a better interpretability both PC scores are presented as score line plots in Fig. 6b and c.

Fig. 6b displays the first PC which shows after 45 min a linear increase of the coating layer against process time. After the stationary level of the "preheating" step the HPMC concentration rises from "spraying 1", throughout "spraying 2" until "drying". Reference values of the mean tablet weight at different time points included in Fig. 6b confirm the NIR predicted coating progress throughout the "spraying 2" step. Interestingly, the real-time NIR measurements were found to be more consistent and also more reliable to monitor the coating growth. This can be explained by the fact that the use of tablet weights to determine the growth of a thin coating layer is far from ideal at least during the early process stages, since process-induced changes of tablet properties other than the coating growth are contributing to the tablet weight. These aspects will be discussed in more detail with the development of the PLS model.

Fig. 6c shows the second PC which comprises the tablet moisture trajectory over time. In spite of the disorder of the scores in the "preheating" step the moisture profile can be monitored. The slope in "spraying 1" shows the increase of the moisture content. Then in "spraying 2" the moisture content decreased as the spray rate changed followed by a plateau phase. In the "drying" step the moisture content decreased again, as expected. The reference values obtained from Karl Fischer titration and included in Fig. 6c confirm the NIR trajectory. The corresponding loadings of both PCs are shown in Fig. 6d.

With the PCA model it was possible to visualize the entire coating process in one PC score plot. The different score clusters indicate the change of process parameters and their effect on the tablet characteristics. Even the unexpected change of the spray rate could be directly identified. The clear separation of coating growth and tablet moisture in different PCs enable a real time monitoring.

Based on the results of the PCA model, PLS models for the determination of tablet weight gain, coating growth and tablet moisture content were developed. Details of all quantitative PLS models are summarized in Table 3. Model I represents the quantitative iPLS model for the determination of the tablet weight with calibration samples from all stages of the process including core tablets (using the first three PCs). To minimize the effect of the core tablet weight variability on reference value accuracy, the mean weight of 100 tablets was used at each process step. This model I was tested against in-line NIR data obtained from the same coating process. The corresponding profile is presented in Fig. 7a. The high R^2 of 0.959 and the low predictive error (RMSEP of 0.29 mg) compared to the theoretical net weight gain of the coating growth between successive spray levels (approx. 0.38 mg) indicate that the model built is sufficiently accurate to be used for the determination of tablet weight changes during the coating process.

However, the weight gain profile presented in Fig. 7a clearly demonstrates that the tablet weights reflect not only the coating growth which can be assumed to be linear, but also the changes in process-related physical properties of the core tablets and at the core/coat interface (e.g. attrition-induced weight loss, core/coat interactions including penetration of coating liquid into the core and subsequent swelling, residual moisture, surface roughness, etc.). As NIR reflectance spectra are sensitive to all these tablet characteristics, it is evident that the 3-latent variable PLS weight gain calibration model I is not sufficiently selective to quantify the coating growth of the very thin HPMC coating layer at the early stages of the process. This clearly implies the use of calibration samples from process stages where the tablet weight gain can be assumed to be dominated by the coating growth. Therefore, a 1-latent variable iPLS model II with calibration samples from $\geq$30% coating level for the selective determination of the coating weight was developed and evaluated (Table 3). The high R^2 of 0.963 and the low RMSEP of 0.21 mg demonstrate the validity of the model in the 30–100% coating level, which is the important range for end point determination. The profile in Fig. 7b represents the application of model II against the in-line NIR data. Interestingly, the prediction of the 20% coating level corresponding to a theoretical coating amount of 0.77 mg per tablet was still very accurate. A much lower weight was predicted for the 10% level confirming the aforementioned process-induced changes of the core characteristics (e.g. liquid penetration and swelling) during the initial stages of the coating process.

Model III represents the 2-latent variable calibration model based on Karl Fischer reference values. The results for the prediction of the tablet moisture content are shown in Table 3. Fig. 7c

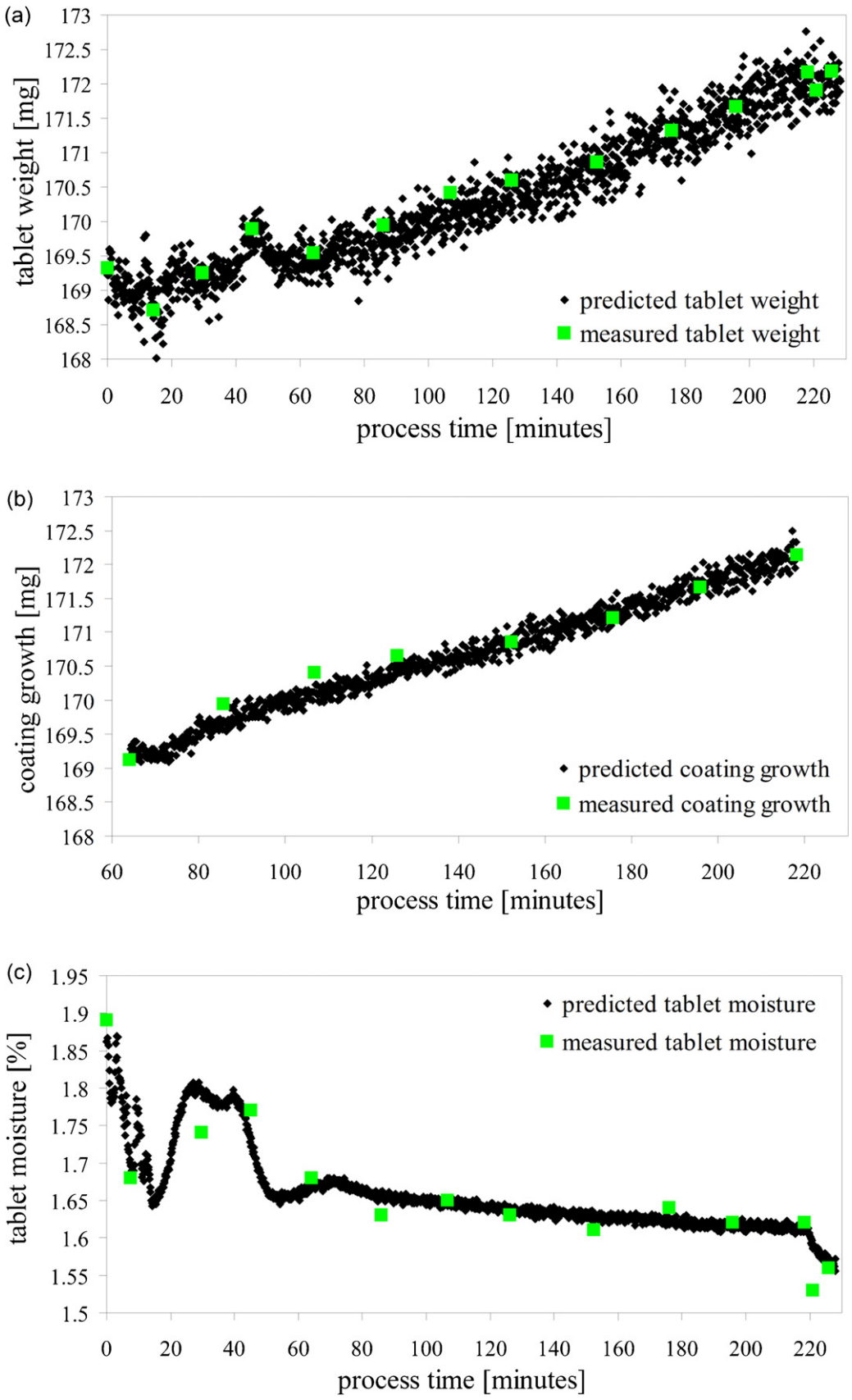

Fig. 7. Real-time application of the quantitative PLS models: (a) model I – tablet weight profile: measured and predicted; (b) model II – coating growth profile: measured and predicted; (c) model III – tablet moisture profile: measured and predicted.

Table 3
Results of PLS calibration models.

Calibration							Prediction		
Target parameter	Model	λ [cm^{-1}]	LV	RMSEC	RMSECV	R^2	RMSEP	R^2	y-Block included sampling range
Tablet weight	I	5646–5508	3	0.20 mg	0.26 mg	0.968	0.29 mg	0.959	All process levels
Coating growth	II	5646–5508	1	0.16 mg	0.24 mg	0.970	0.21 mg	0.963	30–100% coating level
							0.52 mg	0.948	10–20% coating level
Tablet moisture	III	5492–4998	2	0.03%	0.05%	0.921	0.03%	0.911	All process levels

displays its application in the process. The R^2 value of 0.911 and the RMSECV of 4.8e−02% or the RMSEP of 3.1e−02% for the external validation indicate the capability of the method to predict the tablet moisture content during the coating process. The profile shown in Fig. 7c provides further evidence for moisture uptake and swelling of the tablet cores during the initial stages of the coating process.

3.3. Coating thickness determination with Scanning Electron Microscopy (SEM)

Fig. 8a shows the SEM image of the cross section of a coated tablet. The numbers indicate locations of coating thickness measurements. Film thickness determination of water-soluble film coats are challenging because the coatings are very thin and the possibility of interactions with the core is very high, which complicates the measurements.

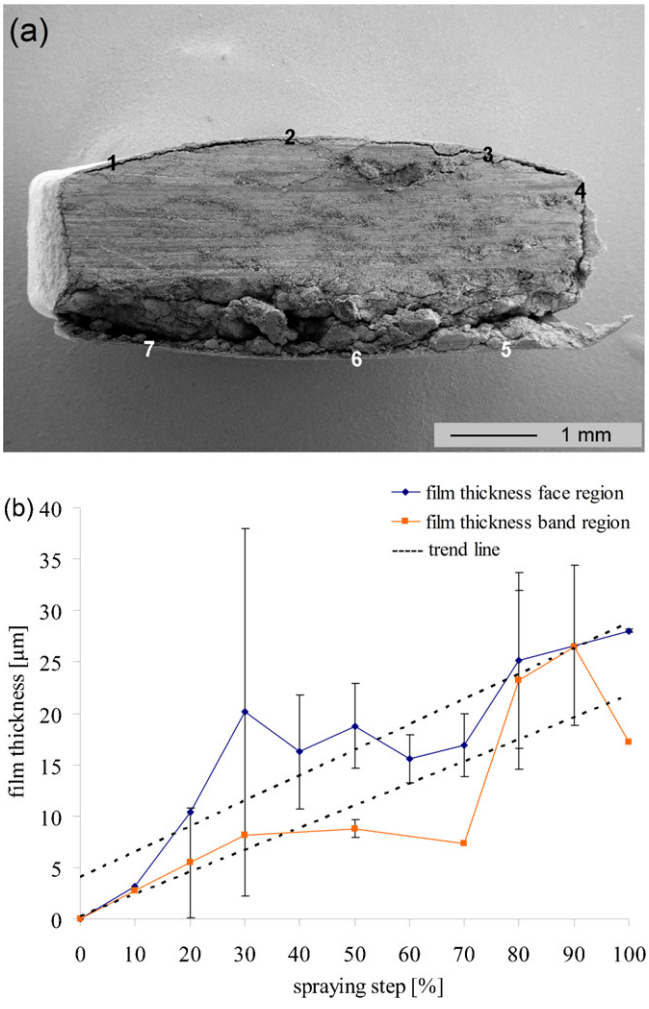

Fig. 8. (a) SEM image of a cross section of a coated tablet. The numbers indicate locations of coating thickness measurements. (b) Comparison of coating thickness in band and face region.

As it was difficult to distinguish between tablet core and coating, EDX spectroscopy was used to ensure where the interface between core and coating could be expected. However, measurements of the coating thickness were still difficult and time-consuming due to the core/coating interactions. Moreover, the limited number of measurements did not allow inter-tablet variability to be determined for both the face and the band region (Fig. 8b). Nevertheless, the trend of the coating thickness increase throughout the different coating steps could be estimated. The standard deviations included in Fig. 8b indicate high intra-tablet variability at the beginning and at the end of the spraying stage, while tablet samples in the middle of the process, i.e. at 40–70% spray level show less variability. Similar observations were made with NIR-CI (see Section 3.4). The mean coating layer thickness of the finished tablets was estimated to be 28 μm in the face region. This clearly confirms the thin coating layer. It turned out that SEM is not an adequate method for the determination of both mean thickness and thickness variability of a thin aqueous based coating on a heart-shaped tablet. As the method is destructive, time-consuming and expensive, it does not allow an easy and fast handling. Hence, NIR-CI was evaluated as an at-line tool to provide more detailed information about the coating growth and uniformity.

3.4. At-line monitoring using Near-Infrared Chemical Imaging (NIR-CI)

To monitor the coating progress in more detail including the spatial distribution of the film coat on the tablet surface, a PLS-2 classification model was built using the whole spectral range. The images of the samples were pre-processed as described in Section 2.2.4. The spectra in the reference library were used as predictors, i.e. two factors were included in the model for the prediction of the core and the HPMC coat, respectively.

Based on the reference library a PLS calibration model was built which was applied to the collected tablet samples. Fig. 9a represents the PLS predicted HPMC images of the tablets, with red pixels being related to high HPMC concentrations and blue pixels indicating low HPMC concentrations. According to this classification there is only little HPMC on the tablet surface after 10% of spraying. The visual inspection of the images reveals, however, a distinct increase of the HPMC concentration throughout the coating process. Thus, monitoring the coating growth with NIR-CI is possible. The PLS predicted images are associated with histogram plots, which were used to perform sample statistic. One parameter given by the histograms is the mean value which was taken to accomplish an Analysis of Variance (ANOVA). Fig. 9b shows a plot with the predicted mean values of the relative abundance of HPMC for each coating step. A continuous increase of HPMC during the spraying steps is evidenced. The results of the ANOVA point out that there is a significant difference between the cores and the coated tablets at the 20% spray level. This confirms the results obtained from the 1-latent variable iPLS model (II) for quantitative in-line NIR monitoring of the coating growth.

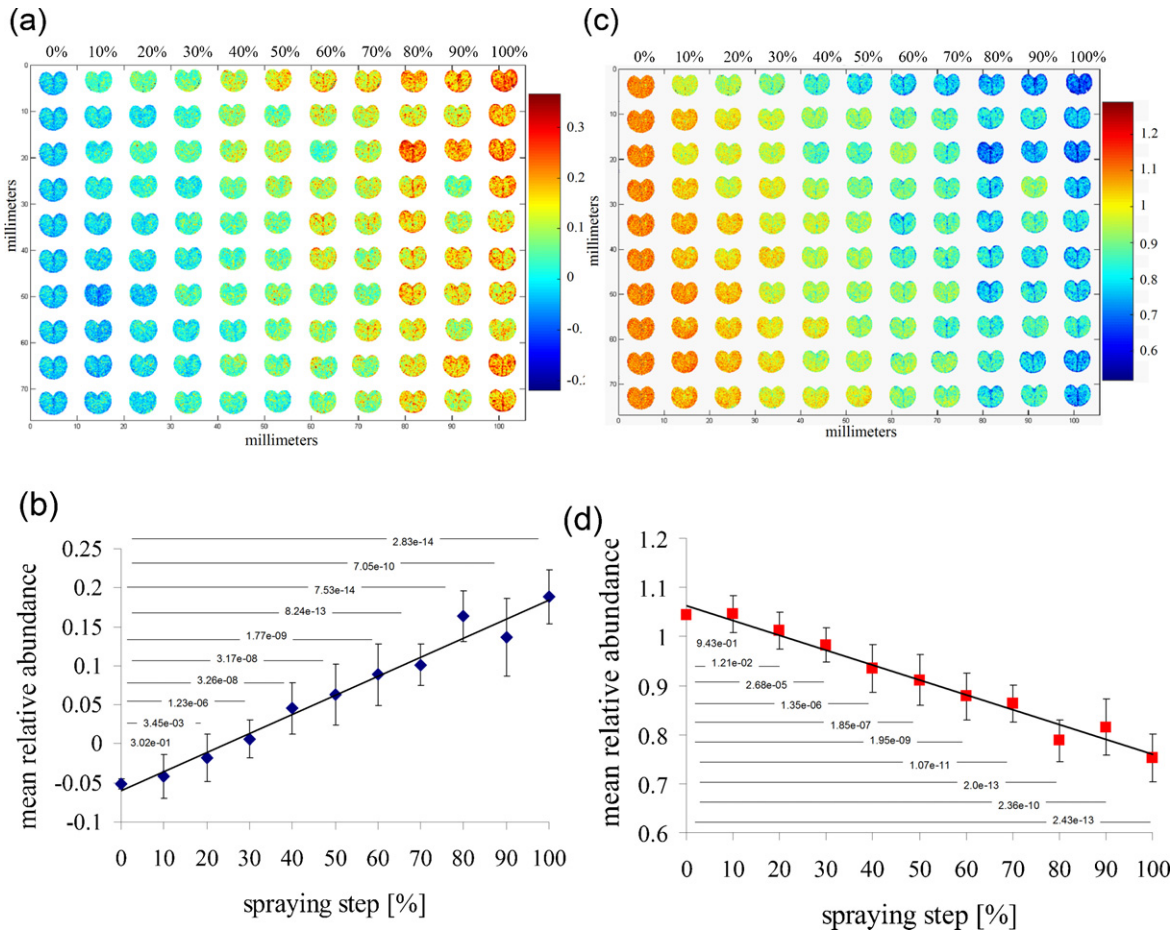

Fig. 9. Concatenated PLS images of tablet samples of 0–100% spraying, showing the growth and variability of the coating layer throughout the process: (a) HPMC predicted images; (b) ANOVA of HPMC mean values; (c) core predicted images; (d) ANOVA of core mean values (the numbers within the intervals demonstrate the calculated *p*-values). (For interpretation of the references to colour in this figure legend, the reader is referred to the web version of the article.)

The coating progress is also visible in the PLS predicted core images of the tablets shown in Fig. 9c. The linear decrease of the mean relative abundance of the core (Fig. 9d) provides further evidence for the coating growth. From the ANOVA results of the PLS predicted images of the cores, which indicate a significant difference between cores and coated tablets at the 10% of spray level, it is obvious that physical changes of the core and/or at the core/coat interface occur during the early stages of the process.

The PLS image analysis enables not only the monitoring of the coating growth, but also the analysis of the spatial distribution of the coating. The distribution of the coating formulation showed strong intra- and inter-tablet variability throughout the process (Fig. 9a and c). In particular, there is higher relative abundance of the coating at the edges and score lines. As expected, this indicates a thicker coating in these regions. A high inter-tablet variability was mainly observed in the beginning and at the end of the coating process. Samples in the middle of the spraying stages present less variability. This could be an indicator for a possible endpoint. The process endpoint determination will be a subject of our future work.

4. Conclusion

The study clearly demonstrated that in-line NIRS is a useful and highly sensitive tool for monitoring in real-time a pan coating process. For a better understanding of the coating process we performed the NIR measurements inside the rotating tablet bed with contact to the product. With the PCA models it was possible to visualize the entire coating process in one plot. The clear separation of each coating step was visible. Also the influence of different process variables on the NIR spectra could be elaborated. Process-induced changes of tablet characteristics were detected and even the time point of the decrease of the tablet bed volume could be identified. A 1-latent variable iPLS weight gain calibration model with calibration samples from ≥30% coating level was sufficiently selective to quantify the coating growth of the very thin HPMC coating layer. The simultaneous determination of process-induced changes of tablet moisture content from NIR in-line spectra could be demonstrated. The PLS predicted image analysis enabled the at-line monitoring of the coating process with NIR-CI. Significant differences between core and coated tablets were detectable after 20% of spraying indicating physical changes at the core/coat interface and coating growth, respectively. Also the coating stages with low inter- and intra-tablet variability could be identified. Overall, this work demonstrated that the new in-line NIRS application in combination with MVDA has the potential to measure the growth of very thin coatings based on materials other than HPMC provided that the NIR signal of the coating material can be separated from other spectral features related to chemical and physical core properties. The combination of in-line NIRS and at-line NIR-CI is an appropriate PAT approach for gaining a better understanding of the tablet coating process thus leading to more effective and robust coating processes and higher product quality.

Acknowledgements

The authors want to thank Dr. Daniel von Bamberg and Dr. Jens Schewitz from Merck Serono for their overall support of the project. Furthermore, we want to thank the whole PAT-Team from Merck Serono PAT-Laboratory Darmstadt for their friendly and kind help and scientific discussions. Dr. Robert Mühlhaus and Dr. Hannes Hochreiner (both from Merck KGaA) are acknowledged for the assistance with the analyzer DoE and the support and installation of the NIR analyzer into the coater, respectively. Also we would like to thank Dr. Norbert Fichtner and his SEM-Team.

References

[1] L.X. Yu, Pharm. Res. 25 (2008) 4.
[2] S. Obara, J.W. McGinity, Int. J. Pharm. 126 (1995) 1–10.
[3] R. Müller, P. Kleinebudde, AAPS PharmSciTech 8 (2007), Article 3.
[4] A.M. Twitchel, Studies on the role of atomization in aqueous tablet film coating, PhD thesis, De Montfort University, Leicster, UK, 1990.
[5] G. Perfetti, T. Aphazan, P. van Hee, W.J. Wildeboer, G.M.H. Meesters, Eur. J. Pharm. Sci. 42 (2011) 262–272.
[6] International Conference on Harmonisation, ICH Q8 (R2): Step 4 (2009).
[7] International Conference on Harmonisation, ICH Q9: Step 4 (2005).
[8] International Conference on Harmonisation, ICH Q10: Step 4 (2008).
[9] http://www.fda.gov/downloads/Drugs/GuidanceComplianceRegulatory Information/Guidances/ucm070305.pdf (2004).
[10] T. De Beer, A. Burggraeve, M. Fonteyne, L. Saerens, J.P. Remon, C. Vervaet, Int. J. Pharm. (2011), doi:10.1016/j.ijpharm.2010.12.012.
[11] G. Reich, Adv. Drug Deliv. Rev. 57 (2005) 1109–1143.
[12] J.D. Kirsch, J.K. Drennen, J. Pharm. Biomed. Anal. 13 (1995) 1273–1281.
[13] J.J. Moes, M.M. Ruijken, E. Gout, H.W. Frijlink, M.I. Ugwoke, Int. J. Pharm. 357 (2008) 108–118.
[14] J.D. Kirsch, J.K. Drennen, Pharm. Res. 13 (1996) 2.
[15] M. Andersson, M. Josefson, F.W. Langkilde, K.-G. Wahlund, J. Pharm. Biomed. Anal. 20 (1999) 27–37.
[16] M. Andersson, S. Folestad, J. Gottfries, M.O. Johansson, M. Josefson, K.-G. Wahlund, Anal. Chem. 72 (2000) 2099–2108.
[17] M.-J. Lee, C.-R. Park, A.-Y. Kim, B.-S. Kwon, K.-H. Bang, Y.-S. Cho, M.-Y. Jeong, G.-J. Choi, J. Pharm. Sci. (2009), doi:10.1002/jps.21795.
[18] M.-J. Lee, D.-Y. Seo, H.-E. Lee, I.-C. Wang, W.-S. Kim, M.-Y. Jeong, G.J. Choi, Int. J. Pharm. 403 (2011) 66–72.
[19] J.D. Perez-Ramos, W.P. Findlay, G. Peck, K.R. Morris, AAPS PharmSciTech 6 (1) (2005), Article 20.
[20] M. Römer, J. Heinämäki, C. Strachan, N. Sandler, J. Yliruusi, AAPS PharmSciTech 9 (2008) 1047–1053.
[21] C. Gendre, M. Genty, M. Boiret, M. Julien, L. Meunier, O. Lecoq, M. Baron, P. Chaminade, J.M. Péan, Eur. J. Pharm. Sci. (2011), doi:10.1016/j.ejps.2011.04.017.
[22] P. Seitavuopio, J. Heinämäki, J. Rantanen, J. Yliruusi, AAPS PharmSciTech 7 (2) (2006), Article 31.
[23] M. Ruotsalainen, J. Heinämäki, H. Guo, N. Laitinen, J. Yliruusi, Eur. J. Pharm. Biompharm. 56 (2003) 381–388.
[24] G. Reich, Pharm. Ind. 64 (2002) 870–874.
[25] L. Maurer, H. Leuenberger, Int. J. Pharm. 370 (2009) 8–16.
[26] S. Zhong, Y.-C. Shen, L. Ho, R.K. May, J.A. Zeitler, M. Evans, P.F. Taday, M. Pepper, T. Rades, K.C. Gordon, R. Müller, P. Kleinebudde, Opt. Lasers Eng. 49 (2011) 361–365.
[27] European Pharmacopoeia, 5th ed., EDQM, Strasbourg, 2005, pp. 59–63 (Chapter 2.2.40).
[28] L. Norgaard, A. Saudland, J. Wagner, J.P. Nielsen, L. Munk, S.B. Engelsen, Appl. Spectrosc. 54 (2000) 413–419.
[29] M.K. Boysworth, K.S. Booksh, in: D.A. Burns, E.W. Ciurczak (Eds.), Handbook of Near-Infrared Analysis, 3rd ed., CRC Press Taylor & Francis Group, Boca Raton/London/New York, 2008, pp. 207–229.